Paleobiology

www.cambridge.org/pab

Article

Cite this article: Salcido, C. J., and P. D. Polly (2025). Parallelism of mandibular function in therian carnivores: a morphometric, phylogenetic, and finite element analysis. Paleobiology, 1-17. https://doi.org/10.1017/pab.2025.10068

Received: 24 May 2024 Revised: 30 July 2025 Accepted: 05 August 2025

Handling Editor: Matthew McCurry

Corresponding author:

Charles Joseph Salcido; Email: csalcido@alumni.iu.edu

© The Author(s), 2025. Published by Cambridge University Press on behalf of Paleontological Society. This is an Open Access article, distributed under the terms of the Creative Commons Attribution licence (http:// creativecommons.org/licenses/by/4.0), which permits unrestricted re-use, distribution and reproduction, provided the original article is properly cited.







Parallelism of mandibular function in therian carnivores: a morphometric, phylogenetic, and finite element analysis

Charles J. Salcido^{1,2} o and P. David Polly o

¹Earth and Atmospheric Sciences Department, Indiana University, Bloomington, IN 47405, U.S.A. ²SWCA Environmental Consultants, Inc., Salt Lake City, Utah 84111, U.S.A.

Abstract

The evolution of the mandible in mammalian carnivores is influenced by ecological demands that have changed over their phylogenetic history. We combined geometric morphometrics and biomechanical analysis (including beam analysis and finite element analysis, or FEA) to assess the interaction between form and function as the mandible has adapted independently to carnivorous diets in therian clades including Metatheria, Mesonychia, "Creodonta," and Carnivoramorpha. Our goal was to determine the relative contributions of mechanical advantage, mandibular force, and mandibular resistance to bending and torsion, to the evolution of mandibular shape in these groups, as well as whether they produce differential rates of shape evolution in the horizontal and ascending rami, which respectively are the tooth-bearing and muscle-loading parts of the structure.

We found that the ascending ramus has higher rates of evolution than the horizontal ramus, making it the more rapidly evolvable portion of the mandible. Statistical evaluation supports this interpretation, as mechanical advantage and resistance to force explain more of the variance in shape than do the beam mechanic estimates that are heavily influenced by the mandibular body. Regression analysis shows that the evolution of specialized carnivory was associated with stronger mandibles in which mandibular shape changed by shortening and thickening of the mandible, increasing the areas of muscle attachment, and increasing the carnassial blade length. Principal component analysis of mandibular shape shows that different clades in Theria have been able to fill out similar specialized carnivorous niches with similar functional metrics despite having different mandibular morphologies.

Non-technical Summary

The evolution of the mandible in mammalian carnivores is influenced by various demands in ecology in different groups. Previous work has tried to quantify the shape of the mandible of certain groups of mammalian carnivores to relate it to different ecologies. In this study, we quantify the shape of the mandible of a larger variety of carnivores and make biomechanical measurements of the mandible to understand the influences of biomechanical properties on mandibular shape and carnivorous mammal ecology and what portions of the mandible undergo the most change over evolution. We define shape by using geometric morphometrics, which quantify a shape based on aligned Cartesian coordinates. Biomechanical measurements used included measuring the relative bite force transmitted, the potential strength of the mandible against bending and torsion in different directions, and resistance of the mandible to stress and strain.

We found that the muscle-bearing portion of the mandible has higher rates of evolutionary change than the tooth-bearing portion. This is supported by statistical tests of the biomechanical measurements that include that portion of mandibular shape and are better correlated with mandibular shape. In the trend of becoming more carnivorous, mammals evolve stronger mandibles that are shortened and thickened with greater areas of muscle attachment and a longer shearing area of the teeth. While looking at the shape variation in mandibles, different groups of mammalian carnivores have been able to fill out specialized carnivorous diets with similar functional metrics despite having different mandibular shapes.

Introduction

Among many clades of Mammalia there have been parallel adaptations to a carnivorous ecology that produced stereotypical changes in jaw shape that are inferred to represent increased functional performance of the mandible for capturing and processing prey (Radinsky 1982; Greaves 1985; Werdelin and Gittleman 1996; Van Valkenburgh 1999, 2007). Phylogenetically distant carnivorous clades, such as metatherian and eutherian carnivores, may have different



constraints on specific jaw shapes (Losos 2011; Renvoisé et al. 2017). However, in principle, the parallel changes in jaw shape with the evolution of carnivory are expected to require similar functional performance such as amounts of stress and strain on the jaw for the typical external forces that occur during prey capture or food processing. We might therefore expect that phylogenetically distant carnivorous mammals may have overall different jaw shapes but with similar lever proportions and loadings on teeth and joints (Van Valkenburgh 1999, 2007; Goswami et al. 2011; Losos 2011; Tseng 2013). Similar functional properties may also be found in food processing mechanics combined with differences in prey capture mechanics that could differentially affect loading on the canines versus the carnassial and molars (Biknevicius and Ruff 1992; Meachen-Samuels and Van Valkenburgh 2009; Slater et al. 2009; Kitchener et al. 2010). In this paper, we will contrast the evolution of the mandibular shape with its functional performance measured by biomechanical efficiency in response to the acquisition of specific dietary specializations in carnivorous mammals.

Some adaptations for increased carnivory in Mammalia include the development of a carnassial shear in which at least one upper tooth and one lower tooth occlude to create a shearing surface that better processes meat (Butler 1946; Crompton and Hiiemae 1969; Greaves 1983; Ungar 2010), often positioned near the midpoint in the mandible to get the most efficient muscle force without trading off gape size (Greaves 1983). For groups that have become more specialized in carnivory, additional adaptations often include reduced mandible length that is often accompanied by a reduction of either anterior premolars or posterior molars as a by-product of selection. This reduction in mandible length increases the efficiency of the lever arm of the mandible adductor complex (Martin 1989; Hunt 1998; Van Valkenburgh 2007; Christiansen 2008). However, this reduction in length is not a ubiquitous trait in all specialized carnivores (e.g., *Ursus martimus*) and longer craniofacial structure may be a by-product of increasing size (Mitchell et al. 2024; Sansalone et al. 2024). Other typical adaptations include increased origin and insertion areas of the temporalis muscle at the temporal fossa and sagittal crest of the cranium (origins) and coronoid process of the mandible (insertion) to produce a stronger or faster bite (Tseng and Wang 2010; Meloro and O'Higgins 2011; Meloro et al. 2015; Hartstone-Rose et al. 2019). Different clades repeatedly evolved into carnivorous forms and ecologies during the Cenozoic (Martin 1989; Van Valkenburgh 1991, 2007). As these clades have converged to fill in the same ecological roles, similarities in their adaptations and how these adaptations have developed are expected to be similar based on presumed linkage of dietary ecology and biomechanical performance and to be seen through functional morphological metrics.

The analyses in this paper will focus on the morphological and functional transitions among four carnivorous diet types: hypocarnivory, mesocarnivory, hypercarnivory, and osteophagus hypercarnivory. Mesocarnivory describes an animal-dominant omnivory, in which more than half of the diet is meat but a noticeable portion is supplemented with non-vertebrate food including insects and plant material (in living taxa, this can be described quantitatively as 50–70% of the diet being composed of meat; Van Valkenburgh 1991, 1999, 2007; Roemer et al. 2009; Balisi et al. 2018). Additionally, most mesocarnivores are typically small to medium body size and hunt prey smaller than themselves. Hypocarnivory describes "true" omnivory, in which half of the diet is composed of meat and the rest is supplemented with nonvertebrate food (in living taxa, this can be described quantitatively as less than or equal to 50% of the diet being composed of meat)

(Van Valkenburgh 1988, 1999, 2007). Hypocarnivores can vary in body size and can be described as "plant-dominated omnivores" due to their wide diet range that includes more plant material. Hypercarnivory describes a diet of carnivores in which entirely or nearly all of the diet is composed of vertebrate meat (in living taxa, this can be described quantitatively as greater than 70% of the diet being composed of meat; Van Valkenburgh 1988, 1991, 1999, 2007; Van Valkenburgh et al. 2004). Hypercarnivores vary in body size and can hunt prey that is equal to or larger in body size than they are. Osteophagus hypercarnivores (e.g., the spotted hyena [Crocuta crocuta]; the extinct bone-crushing dog [Borophagus]) are a subset of hypercarnivores whose diet includes large bones as well as vertebrate meat (Van Valkenburgh 1991, 2007). Hypocarnivory, hypercarnivory, and osteophagus hypercarnivory are typically considered specialized or derived forms of dietary ecology from a mesocarnivorous or insectivorous ancestral condition. The functional differences among these dietary categories are through the differences in the proportion of crushing and slicing features in the dentition (Butler 1946; Crompton and Hiiemae 1969; Greaves 1985; Van Valkenburgh 1991, 1999). While these categories were originally used for the description of extant species, paleontologists have assigned extinct species to them based on functional morphological properties of their teeth, including the development and length of the shearing blades (Butler 1946; Greaves 1983; Van Valkenburgh 1991, 1999, 2007), the area of the crushing basins in the molars (Van Valkenburgh 2007), and structural properties of the teeth such as the microscopic patterns of the enamel (Stefen 1997; Tseng 2013; Tseng and Flynn 2015).

During the Mesozoic Era, the ancestors of carnivorous mammal groups generally occupied insectivore or generalist roles with only a few becoming truly carnivorous consumers of vertebrate flesh or bone (Halliday and Goswami 2016; Benevento et al. 2019). However, in the aftermath of the Cretaceous-Paleogene extinction, many groups of therian mammals (including both placentals and marsupials) began to fill in the roles of secondary consumers and apex predator guilds in ecosystems following the vacancy of non-avian dinosaurs (Halliday and Goswami 2016). The therian mammal clades of Metatheria, Mesonychia, Oxyaenodonta, Hyaenodonta, and Carnivoramorpha occupied guild ecotypes, including mesocarnivores, hypocarnivores, hypercarnivores, and osteophagus hypercarnivores (Van Valkenburgh 1991, 1999; Tseng 2013; Tseng and Flynn 2015). Metatheria includes crown Marsupialia and their closest relatives. Mesonychia is a clade of early predatory mammals within Ungulata that has been inferred at times to be related to whales (Szalay 1969; Solé et al. 2018). Oxyaenodonta comprises the extinct short-faced carnivore group with two pairs of carnassial teeth common in the early Paleogene. Hyaenodonta is the extinct long-faced carnivore group of the Paleogene and early Neogene that has three pairs of carnassial teeth; with Oxyaenodonta, it makes up the potentially polyphyletic clade of "Creodonta" based on the presence of having more than one pair of carnassial teeth (Butler 1946; Borths et al. 2016; Ahrens 2017). Finally, Carnivoramorpha includes crown Carnivora, the paraphyletic "Miacidae," and its closest relatives in Viverravidae (Wozencraft 1989; Wesley-Hunt and Flynn 2005; Spaulding and Flynn 2012; Fig. 1). During the Cenozoic, clades iteratively occupied carnivorous ecotypes in cycles of evolutionary boom and bust. Examples of such replacements include the early Cenozoic Mesonychia and Oxyaenodonta being replaced by Hyaenodonta and Carnivora by the Eocene-Oligocene, Hyaenodonta being replaced by Carnivora by the Oligocene-Miocene,

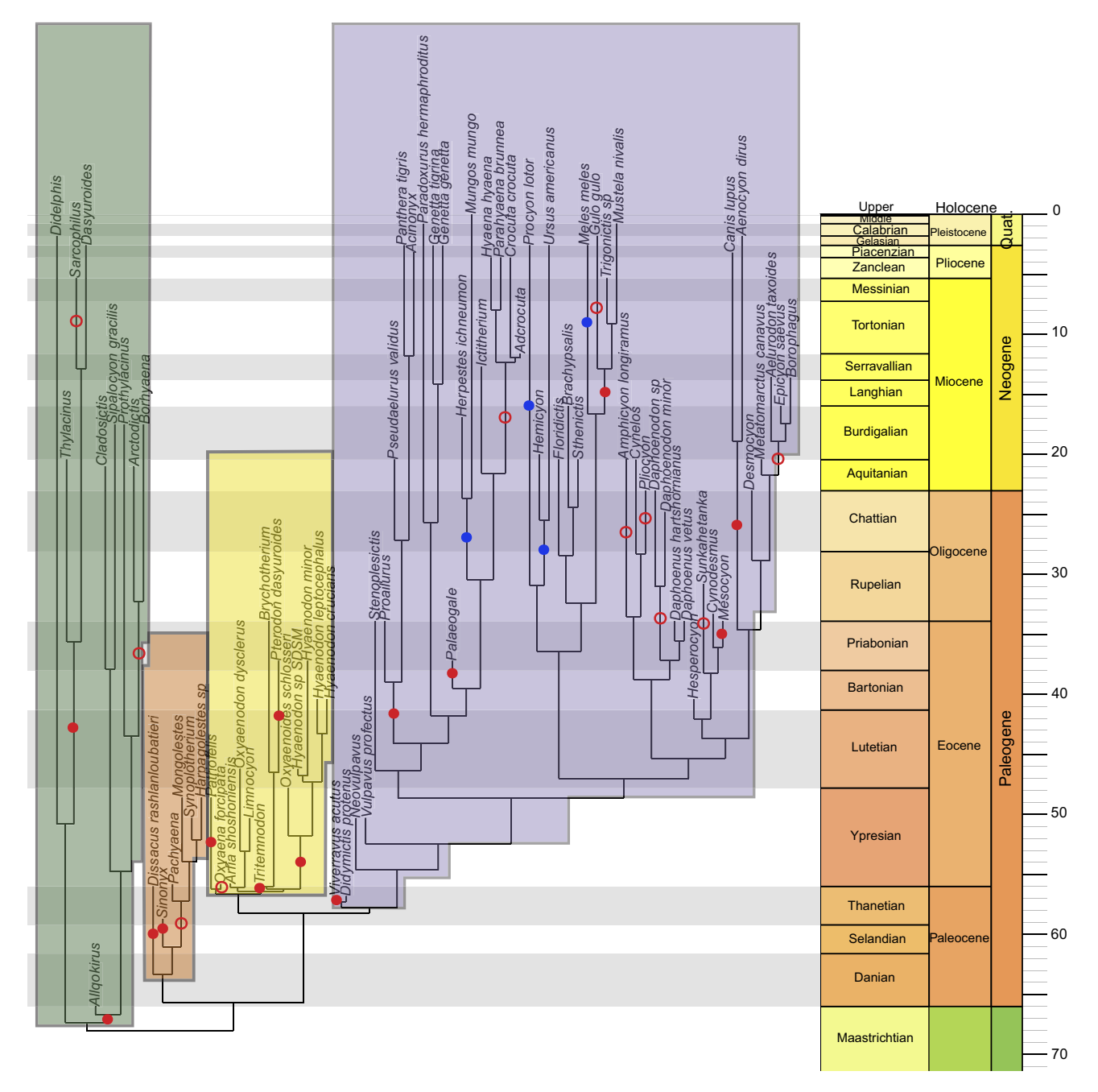


Figure 1. Time-calibrated phylogeny of carnivorous Cenozoic therian mammals with major clades o.f interest highlighted. Green is Metatheria, orange is Mesonychia, yellow is "Creodonta," and purple is Carnivoramorpha. Red dots indicate branches where evolution of hypercarnivory (closed) or bone-cracking hypercarnivory (open) occurs, with taxa to the right of the circles being either hypercarnivores or bone-crackers. Blue dots indicate branches where evolution of hypocarnivory occurs, with taxa to the right of the circles being hypocarnivores. Taxa on the left of red or blue circles are mesocarnivores. Ahrens (2017), Baskin (1998), Borths et al. (2016), Goin et al. (2016), Solé et al. (2018), Spaulding and Flynn (2012), and Wozencraft (1989) were the trees used, with first- and last-appearance dates from the Paleobiology Database (Peters and McClennen 2016). The tree was constructed using the phytools v. 1.5-1 R package (Revell 2023).

and various families within Carnivora replacing each other from the Miocene to the present (i.e., the various subfamilies of Canidae in North America; Martin 1989; Van Valkenburgh 1999, 2007).

Regardless of whether the turnover between the groups was actively produced by competition or passively the result of the filling of niches vacated by extinction, the consequence is that several phylogenetically different groups have independently acquired parallel carnivorous specializations several times in the

history of mammals. Some of the similar adaptations for these ecotypes include the evolution of at least one pair of carnassial-shear teeth that progressively occupied a greater portion of the jaw instead of crushing areas of molars to better process meat (Greaves 1983; Meloro and Raia 2010) and changes in mandibular or cranial shape to catch prey or resist stress from larger struggling prey (Goswami et al. 2011; Prevosti et al. 2012). Van Valkenburgh (2007) describes a series of eco-morphotype convergences among

the members of Carnivora, such as cat-like and hyaena-like morphotypes between feliforms and caniforms, with further morphological convergences, such as the domed cranium of the latter. However, there are noticeable differences within the dental and mandibular morphologies of these groups due to their phylogenetic history. Among these are the larger number of carnassial pairs of teeth in metatherians and creodonts versus carnivorans (Van Valkenburgh 1999, 2007), the lack of "true" carnassial teeth in mesonychians due to their omnivore—herbivore ancestry and the loss of the shear facets on their molars (Szalay 1969; Halliday et al. 2017; Solé et al. 2018), and a larger head-to-body size ratio among non-carnivoramorphans (Van Valkenburgh 1988, 1999; Martin 1989).

Despite the phylogenetic differences in the mandibular shape of these disparate carnivore groups, it stands to reason that the average stress and strain on the mandible should be similar if the diet has similar composition. For example, a species with an osteophagus diet should have a mandible that is better able to resist high levels of stress and strain generated by reaction force from biting on a hard object. We can thus expect a kind of "many-to-one mapping" (Alfaro et al. 2005; Wainwright et al. 2005), in which many mandibular shapes achieve the same functional performance for a limited number of carnivorous diet types. To test this hypothesis, this study uses a combination of geometric morphometrics and biomechanical analyses to test the relationship between form and function in a representative sample of mesocarnivores, hypocarnivores, hypercarnivores, and osteophagus hypercarnivores from across Mammalia. Geometric morphometrics define and quantify the morphology of the mandible, and biomechanical analyses quantify its functional performance. Statistical analyses are then used to determine how the biomechanical variables contribute to variance in mandibular shape. Measurements from biomechanical analyses include beam analysis of the mandibular body, mechanical advantage of the mandible, and finite element analysis of the mandible during biting. We expect that species that are ecologically similar will have similar patterns of stress and strain on the mandible, even if they plot separately on mandibular morphospace, and for the derived groups, we expect that there should be convergence in the stress and strain metrics, which we will confirm with convergence tests.

Materials and Methods

Specimens

A total of 93 specimens, each representing a different species of therian mammal, were used in this study, of which 35 are from extant taxa and the others from extinct taxa. The taxonomic breakdown is as follows: Caniformia (35 species), Feliformia (22 species), and Carnivoramorpha outside of crown Carnivora (4 species) (for a total of 61 carnivoramorphans); Hyaenodonta (11 species) and Oxyaenodonta (2 species) (for a total of 13 "creodonts"); Mesonychia (6 species); and Metatheria (13 species). This selection picks representatives of different points in the evolution of hypercarnivory and/or osteophagy (otherwise known as bone-cracking) behavior in the clade Theria over the course of its evolution, with a sampling of as many independent clades that evolved hypercarnivory or osteophagy. Extant taxa were chosen to represent as many independent transitions as possible from mesocarnivory to hypercarnivory, with the criterion being that at least one hypercarnivore and one mesocarnivore with well-preserved mandibles were available. Extant hypocarnivorous taxa were included to provide outliers

that could potentially be different from mesocarnivores and hypercarnivores. Each species is represented by a single adult mandible as determined by having full permanent dentition. Fossil mandibles are often missing the condyle, coronoid process, or key teeth, and in some cases, our sampling of fossil taxa was constrained by the availability of complete or near-complete mandibles that were not taphonomically deformed

The ecological group breakdown is 36 mesocarnivorous taxa, 30 hypercarnivorous taxa, 21 bone-cracking taxa, and 6 hypocarnivorous taxa (Supplementary Table S1). We have adopted the categorizations used by taxon specialists and assigned them based om previous publications that either describe the diet of extant taxa or are inferred for extinct taxa based on dental morphological descriptions. Our analyses here are of the mandible itself and will avoid mandible morphological descriptions used to determine whether taxa are mesocarnivorous, hypercarnivorous, hypercarnivorous bone-crackers, or hypocarnivores, so the mandibular analyses here are independent of the morphological criteria used for dietary categorization. All taxa are represented and studied via photographs taken from collection databases and previous publications or taken directly during visits.

Institutional Abbreviations. AMNH: American Museum of Natural History, USA; BMNH: Natural History Museum, London (formerly the British Museum of Natural History), UK; CGM: Egyptian Geological Museum, Egypt; CORD-PZ: Museo de Paleontologia, Facultad de Ciencias Exactas, Fisicas y Naturales de la Universidad Nacional deo Cordoba, Argentina; IUPC: Indiana University Paleontology Collections, USA; MHNC: Museo de Historia Natural "Alcide d'Orbigny," Bolivia; MHNT.PAL: Muséum d'Histoire Naturelle de Toulouse, France; MNHN: Museum National d'Historie Naturelle, France; MPM-PV: Museo Regional Provincial "Padre M. J. Molina," Argentina; UF: University of Florida, USA; UMMZ: University of Michigan Museum of Zoology, USA; USNM: Smithsonian Institution National Museum of Natural History, USA; YPM: Yale Peabody Museum, USA.

Geometric Morphometrics

Geometric morphometrics is the analysis of shape that uses Cartesian landmark and semilandmark coordinates to capture variation in shape (Adams et al. 2004). Landmarks for geometric morphometrics were collected from photographs using the multipoint tool in the software ImageJ (Rasband 1997). Images were processed to have the rostrum of the mandible pointing toward the left side of the photograph. Fifteen landmarks were taken from the mandible, including (1) the anterior and (2) posterior of the canine root, (3) the anterior and (4) posterior of the premolar row, (5) the projection of the protocone cusp of the "principal" carnassial or its geometric equivalent (which will be referred to throughout this paper simply as the "carnassial"), (6) the posterior of the molar row, (7) the tip of the coronoid process, (8) the highest and (9) lowest points of the condylar process, (10) the angular notch between the angular process and the condylar process, (11) the angular extreme of the angular process, (12, 13, and 14) the perpendicular point on the ventral side of the mandibular corpus (from 6, 4, and 2, respectively) based on the horizontal line between landmarks (1) and (6), and (15) the most anterior point of the masseteric fossa (Fig. 2). These landmarks follow Meloro and O'Higgins (2011).

Geometric morphometric analysis was carried out in R (Ihaka and Gentleman 1996) with the R package geomorph v. 4.0.5 (Adams and Otárola-Castillo 2013; Adams et al. 2023). Outlines were

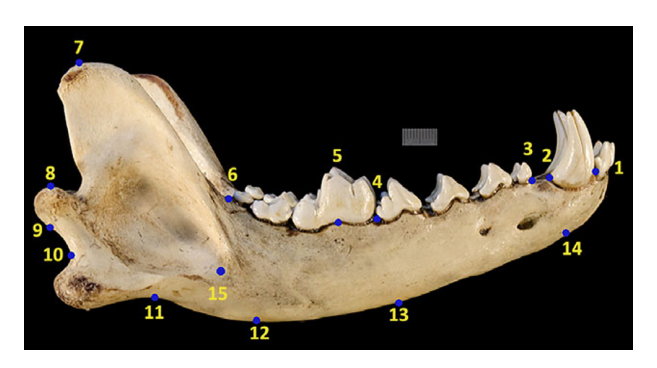


Figure 2. Landmark scheme of the therian mammal jaws in this analysis with a *Canis lupis* mandible as an example obtained from the University of Michigan Museum of Zoology Animal Diversity Web database.

imported into rStudio after processing into a TPS format. Landmarks were Procrustes superimposed to align landmarks and eliminate the difference in size so that variation in landmark placement and shape can be meaningfully analyzed. The aligned shapes underwent principal component analysis (PCA) to identify the major axes of shape variation in the sample and to provide a new set of shape variables that are mathematically uncorrelated with one another. Procrustesaligned shapes also went through a single-factor multivariate analysis of variance (MANOVA; Adams and Collyer 2018; Huberty and Petoskey 2000) of ecological categories and taxonomic grouping (Adams and Collyer 2018) to compare correlation of shape between the two. To determine whether any of the ecological groups are morphological outliers, we compared Procrustes distances between their shapes and calculated an unweighted pair group method with arithmetic mean (UPGMA) tree to show their differences. Morphological integration analysis was performed to test which parts of mandibular shape are modularized and independently evolving. Comparative morphological shape evolution of the horizontal ramus (the tooth-bearing body of the mandible) and the ascending ramus (the posterior portion of the mandible consisting of the coronoid, condylar, and angular processes) was done using the function compare.multi.evol.rates to see the rates of shape evolution between the areas of mandibular shape identified by the integration analysis. This analysis estimates multivariate evolutionary rates assuming a Brownian motion model of evolution (Denton and Adams 2015). For this analysis, the landmarks were subdivided as landmarks 1-5 and 12-14 for the horizontal ramus and landmarks 6-11 and 15 for the ascending ramus. A time-calibrated phylogenetic tree was used for these analyses derived from Newick trees from Ahrens (2017), Baskin (1998), Borths et al. (2016), Goin et al. (2016), Solé et al. (2018), Spaulding and Flynn (2012), and Wozencraft (1989) that included the taxa from this research. The Spaulding and Flynn (2012) topology was used for the higher-level relationships and the others (Wozencraft 1989; Baskin 1998; Borths et al. 2016; Goin et al. 2016; Ahrens 2017; Solé et al. 2018) for family-level clades. The Newick trees were combined with the R package phytools v. 1.5-1 (Revell 2023) and time-calibrated with first- and last-appearance dates from the Paleobiology Database (Peters and McClennen 2016; Fig. 1) using the timePaleoPhy function.

Beam Analysis and Mechanical Advantage

To compare mandible bite performance at different locations along the toothrow and among taxa, we used principles of beam analysis. Beam analysis describes an object regarding its strength, resistance, and reaction to bending if a force is applied to it as if it were beam (in this case, the mandible is being treated as a beam; Metzger et al. 2005; Therrien 2005; Porro et al. 2011). This analysis was carried out via 2D photographs using methods outlined by (Therrien 2005). Seven measurements were taken as follows to calculate the second moment of area (\it{I}) for the canine, precarnassial, carnassial, and postcarnassial areas of the mandibular body: the dorsoventral height and the labiolingual width. These measurements were taken in ImageJ using the line segment tool from buccal and occlusal photographs of mandibles. These measurements were used to calculate the second moment of area (\it{I}) for each plane:

$$Ix = \frac{\pi ba^3}{4} \tag{1}$$

$$Iy = \frac{\pi ab^3}{4} \tag{2}$$

where a represents the dorsoventral radius and b represents the labiolingual radius. Ix is the second moment of area on the labiolingual plane and Iy is the second moment of area for the dorsoventral plane. The section modulus (Z) of each plane in the area can then be obtained using the equations:

$$Zx = \frac{Ix}{a} \tag{3}$$

$$Zy = \frac{Iy}{h} \tag{4}$$

The section moduli can then be used to determine relative bending force in each area. The dorsoventral bending force (DBF) and the labiolingual bending force (LBF) may be obtained by dividing Zx and Zy, respectively, by the distance of each area to the condyle (L). These values must then be log-transformed to be comparative to one another due to the range of body sizes:

$$DBF = \log\left(\frac{Zx}{L}\right) \tag{5}$$

$$LBF = \log\left(\frac{Zy}{L}\right) \tag{6}$$

Additionally, the section modulus for the x-plane may be divided by the section modulus for the y-plane to give the relative bending force (RBF):

$$RBF = \frac{Zx}{Zy} \tag{7}$$

These bending force values may then be used to generate a bending force profile of the mandibles along the horizontal ramus from the rostral to posterior end.

Mechanical advantage measurements were used as a proxy for bite force. Mechanical advantage is a ratio of the length of the in-lever (the lever arm producing force, i.e., the muscle) to the length of the out-lever (the lever arm where the force comes out at, i.e., the bite point; Greaves 1983, 1985). Mechanical advantage was calculated for each combination of in-lever for temporalis and masseter muscle and out-lever for the canine and carnassial bite.

Digital Model Creation

We also used finite element analysis (FEA) to estimate bite performance as a measure of stress and strain. To do this, we created 3D

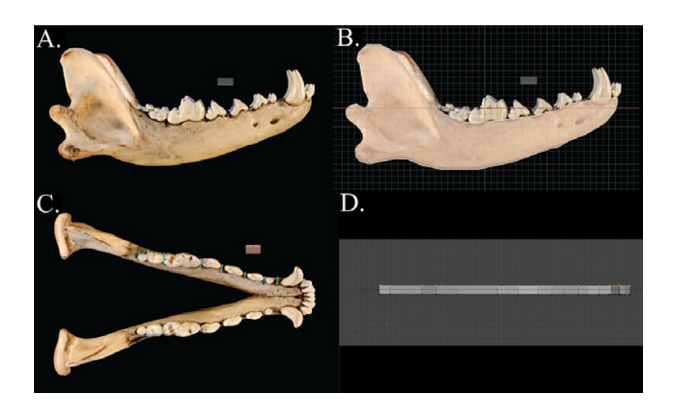


Figure 3. The process of creating a simple extruded 3D finite element model using the *Canis lupus* mandible from Fig. 2 as an example. **A,** A picture of the mandible from the lateral view. **B,** Imported photo from **A** as a background in Blender to trace and then fill in. **C,** From an occlusal view of the mandible, measuring average tooth width to extend traced object to create a simple extruded 3D model in Blender **(D)**.

digital models from each 2D photograph. Before model creation, we took a series of linear measurements from the specimens from buccal and occlusal views of the mandibles, including the length and height of the mandible and the width of each tooth. Simple extruded 3D models were created from a series of photographs based on the methods of Morales-García et al. (2019). This procedure was accomplished by importing photographs and outlines of the buccal view of mandibles into the 3D software Blender (Brito 2007), where a 2D mesh was created via outlining the imported images, which produces a 2D mesh. Our models intentionally represented only the bony mandible and excluded the dentition, because tooth count varies among the different taxa studied, and the completeness of the dentition varied among fossilized specimens. The 2D mesh was then extruded based on the average width of the toothrow measured previously in ImageJ. Simple extruded 3D models were confirmed to be the size of the specimen before being exported. The Blender models were then imported into MeshLab (Cignoni et al. 2008) for remeshing to ensure a watertight mesh with an appropriate number of tetrahedral elements of relatively equal size was created before being exported into the software FEBio for FEA (Maas et al. 2012). The meshing process is illustrated in Figure 3.

Finite Element Analysis

FEA was applied to the resulting 3D extruded mandible models to calculate the stress and strain imposed by bites at two functionally comparable locations along the toothrow. FEA is the use of calculations, models, and simulations to understand how an object may behave when a force(s) is(are) applied to it by treating the model as a number of discrete, connected elements (Richmond et al. 2005; Ross 2005; Rayfield 2007). Simple extruded 3D models were imported into FEBio to determine von Mises stress and strain from the forces of biting and feeding in the mandibles (Morales-García et al. 2019; Varela et al. 2023). Solved finite element models can be used to determine the stress (force/area) and strain (deformation) of an object by calculating the movement of fixed points on a model when a force is applied to it (Strait et al. 2005; Bright and Gröning 2011; Reed et al. 2011). A convergence test on element resolution was done to determine the minimum number of elements necessary that would produce the same results as higher-resolution models (Rayfield 2007; Bright 2014). The minimum number of elements was found to be an average of about 600,000 elements after using the increasing resolution tool in FEBio.

The models were assigned isotropic elastic properties with a density of 1900 kg/m³, Young's modulus of 20 GPa, and a Poisson ratio of 0.3 based on the average values of mammalian cortical bone (Currey 1984; Wroe et al. 2005; Tseng 2013). The whole mandible was assigned these properties. As mentioned earlier, the models were created without the dentition, including tooth roots, because previous studies have shown that uncertainty and variation in the tooth roots introduce biases that make overall comparisons difficult (Marinescu et al. 2005) and have integrated teeth and mandible bodies as one, as they are both stiff (Tseng 2013; Bright 2014; Serrano-Fochs et al. 2015; Morales-García et al. 2019). Because both fossil and extant mandibles are composed of the same tissue, we used the same settings for material properties across the entire mandible in both extant and extinct taxa. So long as all models share the same material properties, results of FEA can be comparable (Rayfield 2007; Wroe 2008; Bright 2014).

To set our analyses up as counter-lever experiments, we placed boundary constraints on the mandibular condyle and the most dorsal and ventral areas of muscle attachment (Tseng et al. 2023). We used multipoint constraints defined with four degrees of freedom (for muscle points: U1 = U2 = U3 = UR1 = UR2 = UR3 = 0; for the mandibular condyle: U1 = U2 = U3 = UR3 = 0; U1 is the mediodistal axis, U2 is the dorsovental axis, and U3 is the axis along the jaw length; U describes translational movement, and UR describes rotational movement) (Tseng 2013; Gill et al. 2014). The mandibular condyle constraints allow only for the expected movement of the joint as it would occur in vivo.

Force loads were placed at the two bite points of interest: the canine and the carnassial. These points were chosen because they are two different points of the mandible (rostral vs. posterior) and have different functions (acquiring/subduing prey with the canine vs. chewing/processing food with the carnassial/molar area). The carnassial is the tooth most associated with the inferred diet and ecology of the mammals in this dataset (Greaves 1983; Pineda-Munoz et al. 2017; Hopkins et al. 2022). *Vulpavus profectus*, a small, non-carnivoran carnivoramorphan and inferred mesocarnivore, was loaded 100 N at either the canine or carnassial. This 100 N load on Vulpavus was then scaled according to surface area of other mandibles to produce a comparable load for other models and allow a comparison of stress and strain on the mandible based on differences in mandibular shape (Dumont et al. 2009). Stress and strain values were recorded as the volumetric average of the von Mises stress and effective Lagrange strain of the entire shape (volumetric average is similar to the mesh-weighted arithmetic mean from Marcé-Nogué et al. [2017]).

Multivariate regression was used to extract the component of shape associated with each of the biomechanical metrics: the mechanical advantage of temporalis and masseteric bites at the canine and carnassial separately; the maximum dorsoventral bending force; the maximum labiolingual bending force and relative mandibular force at the canine, precarnassial, carnassial and postcarnssial areas; and average von Mises stress when biting on the canine and carnassial separately. These regressions tested which biomechanical metric had the highest explanatory power for mandibular shape. A phylogenetic generalized least square (PGLS) was also performed to test the relationship between these metrics and shape, correcting for phylogeny. A multivariate regression of shape onto centroid-size was done to estimate the allometric component of the relationship between mandibular shape and biomechanical variables. Canine stress and carnassial stress underwent a MAN-OVA of ecological and taxonomic categories to analyze the

correlation of the stresses and the categories and was followed by a Tukey post hoc test to assess between-group differences between groups.

Convergence Testing

The degree of convergence was measured using Ct-metrics as outlined in Grossnickle et al. (2024). Ct-metrics are derived from the C-metrics of Stayton (2015) and measure whether the tips of the tree are closer in variable space than their ancestors were. Ct1 is the preferred Ct measure and is calculated as $1 - (D_{tip}/D_{max,t})$, with D_{tip} representing the distance between phylogenetic tips of focal taxa and $D_{\text{max.t}}$ representing the maximum distance between any tips or ancestral nodes of those lineages that has been closed by subsequent evolution. Positive Ct1 indicates convergences, with 1 being total convergence, and negative *Ct1* indicates divergence. This was done with the R function *calConvCt* from the package convevol v. 2.2.1 (Brightly and Stayton 2024). The calConvCt calculates the overall average *Ct*-metrics, group-specific *Ct*-metrics, and the group weighted means Ct-metrics (i.e., averaged giving equal weight to each group pairing as opposed to each taxon pairing so that one large group does not disproportionally influence results). Ct1 measures were acquired to test for convergence in mandibular stress from canine and carnassial bites among derived hypercarnivores and bone-crackers.

Results

Geometric Morphometrics Analysis

The primary differences among the carnivore groups are related to the relative position of the tooth row, the depth of the mandible, and the configuration of the processes at the posterior end. Procrustes distances of all specimens are used in a PCA and plotted onto a PCA plot with polygons around subsets to identify groups (Figs. 4, 5). PC 1 represents primarily the angle of the horizontal ramus of the jaw. Negative PC 1 represents a more angular jaw that is deeper with a thicker condyle. Positive PC 1 is a less angled horizontal ramus that is shallower and has a smaller condyle. PC 2 represents the length of the premolar area (landmarks 3, 4, 13, and 14) and the molar area (landmarks 4, 5, 6, 12, and 13). Positive PC 2 is a more anteriorly positioned premolar area and a larger molar area. Negative PC 2 is a more posteriorly positioned premolar area and a smaller molar with landmarks 4 and 6 coming closer to landmark 5. PC 3 represents the shape of the mandible between canine landmarks (1, 2, 3, and 14) and the molar landmarks (4 and 13) (the premolar row) as well as the closeness of landmark 5 between landmarks 4 and 6. Positive PC 3 has more rostral shift of the premolar row and negative PC 3 is a wider premolar row with landmarks 4 and 6 closer

The PCA shows that species overlap among ecological groups and that different clades have possibly converged on these ecologies but there are some noticeable areas of uniqueness, as seen in Figure 4 (this is supported by a single-factor MANOVA on Procrustes distances with an $R^2 = 0.12$). On the positive half of PC 1, all ecological groups can be found, but mesocarnivores can be found farther along the positive end of the axis toward the periphery. The negative half of PC 1 has all ecological groups, but those categorized as hypercarnivores and bone-crackers are predominantly on this side compared with the positive half of PC 1 and reach farther toward the periphery. For PC 2, the negative end lacks most categorized hypocarnivores (the exception being *Nandinia*) and

has categorized hypercarnivores and bone-crackers reaching farther toward the periphery, while the positive end has all ecological groups, with mesocarnivores reaching the periphery of the axis with Dasyuroides and bone-crackers with Sarcophilus. The negative end of PC 3 has all ecological groups, with most mesocarnivores and all hypocarnivores on this end, and both reach the farthest end of the axis. The positive end of PC 3 has hypercarnivores and bonecrackers reaching toward the periphery of the axis. Hypocarnivores are the most distinctive ecological group, with most being separated from other groups with PC 2 and PC 3 (except Herpestes ichneumon and Nandinia). Hypercarnivores and bone-crackers are the next most distinctive, being separated on PC 2 and PC 3 for the former and PC 1 and PC 2 for the latter, with certain quadrants having little presence (negative PC 2 and positive PC 3 for hypercarnivores and negative PC 1 and PC 2 for bone-crackers). Mesocarnivores generally range around the center of morphospace with more taxa on one end of either PC 1 or PC 3 when looking with PC 2 and mesocarnivorous metatherians pulling it toward the positive end of PC 2. Being near the center could indicate that they possibly define the mean shape. An UPGMA tree of mandibular morphology shows that categorized hypocarnivores are the most different morphologically, and hypercarnivores and bone-crackers are more similar to one another than mesocarnivores (Supplementary Fig. S1).

The same plots are labeled with taxonomic groups in Figure 5, which shows that the hypercarnivores are composed of specialized members of several clades that converged on the same area of morphospace (placental hypercarnivores occupying negative PC 2 morphospace and metatherians in general occupying mostly the quadrant of positive PC 2 and negative PC 1 morphospace). Stem carnivoramorphans occupy a narrow space in negative PC 2 and mostly in positive PC 1. Caniforms and hyaenodonts are primarily around the center of morphospace but with mesonychids slightly off-center mostly in the negative PC 1/PC 2 quadrant. This may be because both clades (except for Limncyoninae in Hyaenodonta and Mongolestes) still retain the plesiomorphic three-molar jaw morphology among placental mammals. Oxyaenids are closer to felids in morphospace. When looking at PC 2 and PC 3, all carnivoramorphs can be primarily separated from non-carnivoramorphs on negative PC 3 and negative PC 2, with mesonychids and oxyaenids between them and the rest of the non-carnivoramorph groups

The subdivided landmarks for the *compare.multi.evol.rates* function show a significant difference in rates of evolution, with ascending ramus having faster rates of shape change versus the horizontal ramus (Fig. 6). This difference in rates of morphological evolution is approximately 1:3 for the ascending versus the horizontal ramus.

Linear Functional Measurements and Beam Analysis

Mechanical advantage and beam analysis metrics of each taxon were regressed onto the Procrustes distances of the respective taxa, showing the former has higher explanatory power (Table 1). R^2 values of each individual were generally less than 0.10. When summed according to each metric category (DBF, LBF, RMF, or mechanical advantage), mechanical advantage has the most explanatory power (0.35) and relative mandibular force has the least explanatory power (0.17). The explanatory power of most of the beam analysis metrics is greatly improved under a MANCOVA when phylogeny is considered. PGLS tests with the mechanical advantage and beam analysis metrics showed increased R^2 values

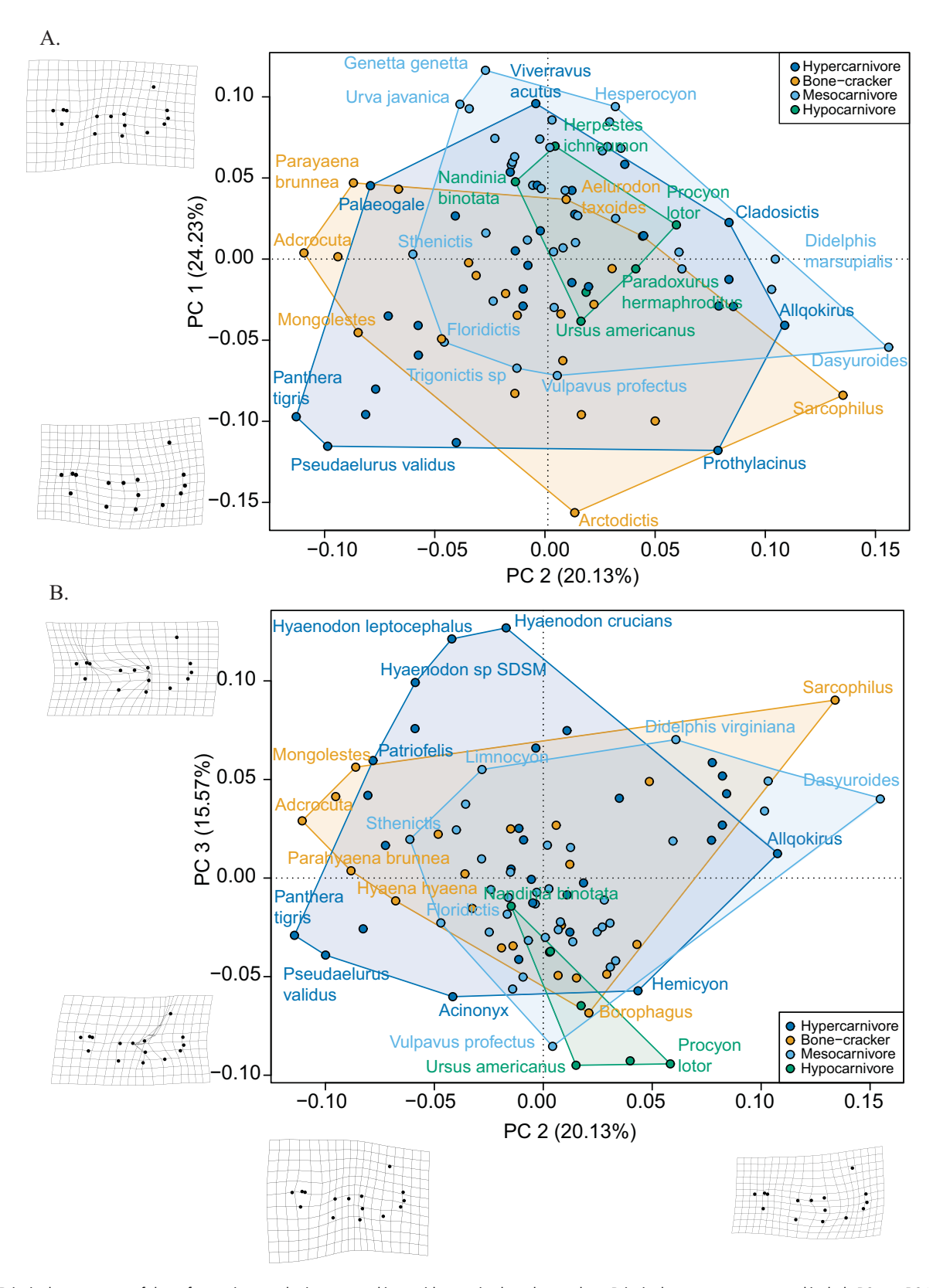


Figure 4. Principal components of shape for carnivorous therian mammal jaws with grouping based on ecology. Principal components compared include PC 1 vs. PC 2 (A) and PC 3 vs. PC 2 (B), keeping PC 2 on the x-axis.

in comparison to the initial regression that were significant except for the RMF of the canine which decreased (Table 2).

The regressed functional metrics are visualized with the landmarked shape to demonstrate the deformation of shape via

splines as each metric increased in value (Fig. 7). The metric with the highest explanatory power is the mechanical advantage of the canine tooth with the temporalis muscle (with the RMF of the canine coming in a close second), and the metric with the least

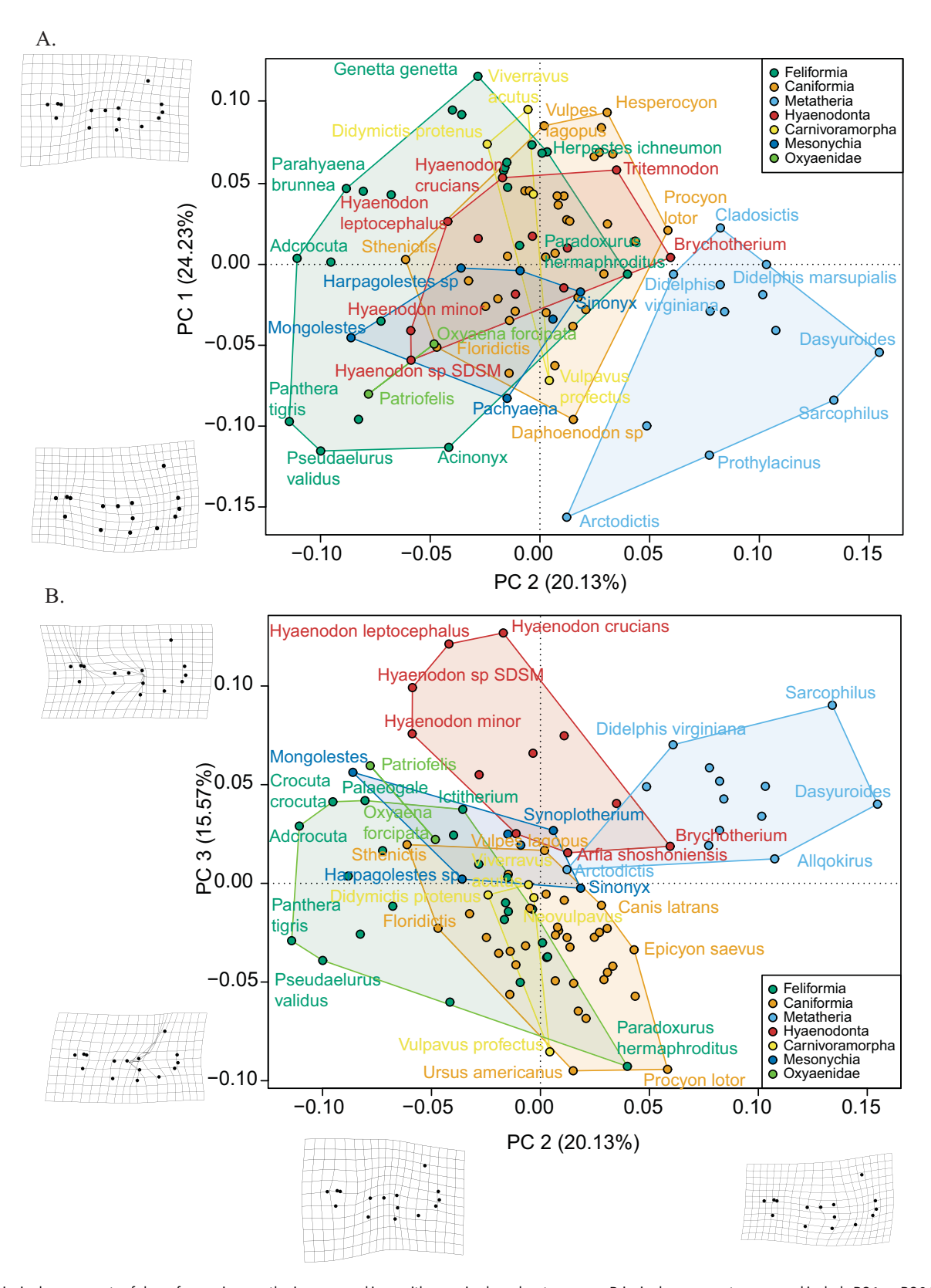


Figure 5. Principal components of shape for carnivorous therian mammal jaws with grouping based on taxonomy. Principal components compared include PC 1 vs. PC 2 (A) and PC 3 vs. PC 2 (B), keeping PC 2 on the x-axis.

explanatory power is the relative mandibular force around the precarnassial area (Table 1). It should be noted that the mechanical advantage of the carnassial and masseter may be indicative of diet, as the taxa with highest values are hypercarnivores, and the taxa

with the lowest values are hypocarnivores. The relative mandibular force of the premolar appears to be somewhat related to body size, as the large metatherian carnivore *Arctodictis* has the highest value, while the much smaller *Allqokirus* has the lowest value. However, a

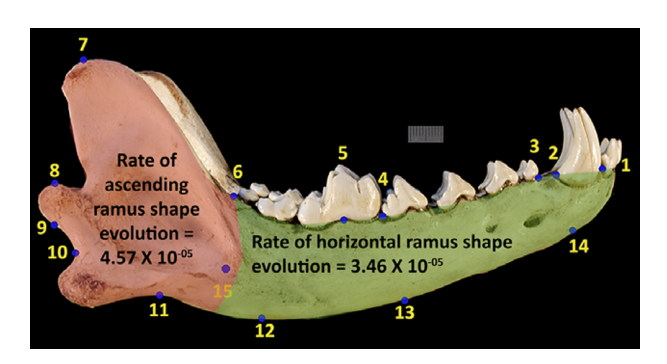


Figure 6. Landmark scheme figure from Fig. 2 but with highlighted areas designating landmarks associated with the ascending ramus in red and the horizontal ramus in green with rates of evolution listed. The ratio of these rates is approximately 1:3.

Table 1. List of p-values and R^2 values of the respective functional metrics regressed onto Procrustes-aligned mandible shape. DBF, dorsoventral bending force (resistance to dorsoventral forces); FES, finite element analysis; LBF, laterolingual bending force (resistant to laterolingual forces); MA, mechanical advantage; RMF, relative mandibular force.

Functional measurement	<i>p</i> -value	R ²
DBF at canine	0.001	0.09
DBF at precarnassial	0.001	0.08
DBF at carnassial	0.001	0.08
DBF at postcarnassial	0.001	0.08
Summed R ²		0.33
LBF at canine	0.001	0.08
LBF at precarnassial	0.001	0.08
LBF at carnassial	0.001	0.08
LBF at postcarnassial	0.001	0.08
Summed R ²		0.32
RMF at canine	0.001	0.10
RMF at precarnassial	0.031	0.02
RMF at carnassial	0.028	0.02
RMF at postcarnassial	0.01	0.03
Summed R ²		0.17
MA canine-masseter	0.001	0.07
MA canine-temporalis	0.001	0.10
MA carnassial-masseter	0.001	0.09
MA carnassial-temporalis	0.001	0.09
Summed R ²		0.35
FEA – stress at canine	0.001	0.14
FEA – stress at carnassial	0.001	0.09
Summed R ²		0.23

multivariate regression of shape on centroid size reveals a weak and nonsignificant effect from allometry on the shape data ($R^2 = 0.02$ and p-value = 0.075). Generally, as biomechanical values increase, mandibles undergo shortening and thickening with increases in muscle attachment areas such as coronoid height and increasing

Table 2. List of p-values and R^2 values of the respective metrics from phylogenetic generalized least squares (PGLS) onto Procrustes-aligned mandible shape. DBF, dorsoventral bending force (resistance to dorsoventral forces); LBF, laterolingual bending force (resistant to laterolingual forces); RMF, relative mandibular force; MA, mechanical advantage.

PGLS regression of functional measurements onto Procrustes-aligned shape results				
Functional measurement	<i>p</i> -value	R^2		
DBF at canine	0.001	0.17		
DBF at precarnassial	0.001	0.15		
DBF at carnassial	0.001	0.14		
DBF at postcarnassial	0.001	0.15		
DBF summed R ²		0.61		
LBF at canine	0.001	0.15		
LBF at precarnassial	0.001	0.13		
LBF at carnassial	0.001	0.12		
LBF at postcarnassial	0.001	0.15		
LBF summed R ²		0.55		
RMF at canine	0.003	0.04		
RMF at precarnassial	0.001	0.07		
RMF at carnassial	0.001	0.10		
RMF at postcarnassial	0.001	0.07		
RMF summed R ²		0.28		
MA canine-masseter	0.001	0.11		
MA canine-temporalis	0.001	0.17		
MA carnassial-masseter	0.001	0.09		
MA carnassial-temporalis	0.001	0.06		
MA summed R ²		0.43		
FEA – stress at canine	0.001	0.25		
FEA – stress at carnassial	0.001	0.10		
FEA summed R ²		0.35		

carnassial blade length (Fig. 7). Masseteric area appears to be more controlled by the posterior side of the dentition than the more rostral side.

Finite Element Analysis

An analysis of variance (ANOVA) shows that the canine stress and strain on the mandibles is significantly different among the different dietary categories of mesocarnivore, hypercarnivore, hypocarnivore, and bone-crackers (*p*-value < 0.05). On average, mesocarnivores have the highest stress from the canine load, followed by hypercarnivores, hypocarnivores, and bone-crackers, and hypocarnivores have the highest stress from the carnassial, followed by mesocarnivores, bone-crackers, and hypercarnivores (Table 3). This difference between these groups is more apparent in stress and strain on loads from the canine bite as opposed to the carnassial bite. Between-group differences are significant in the canine bite stress between mesocarnivores and bone-crackers (adjusted *p*-value < 0.01), and there are no significant differences between groups for the carnassial bite stress (Table 4). In terms of the differences between the different clades, stress and strain on the mandible is

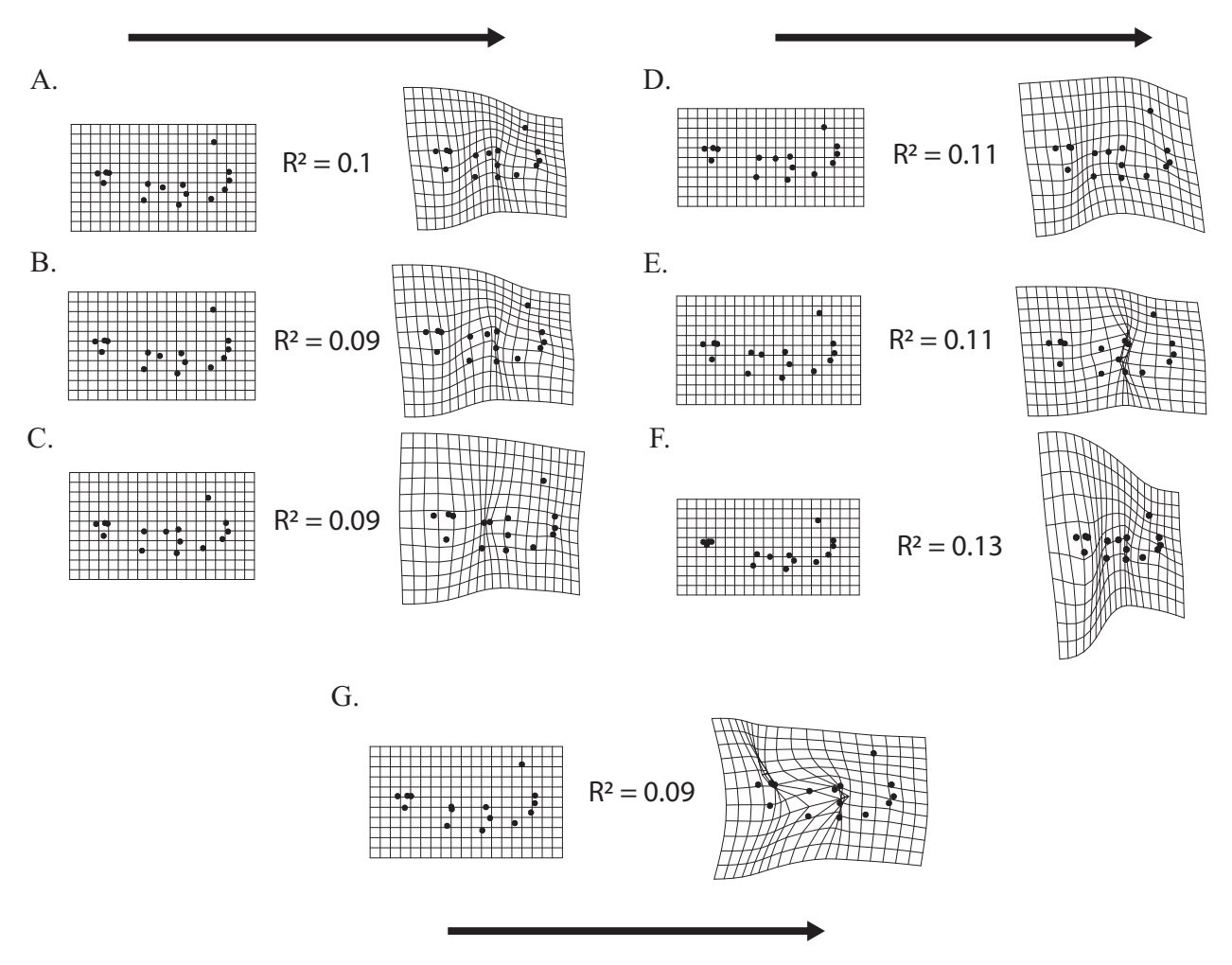


Figure 7. Spline deformations of mandible strength per functional metric with its associated R^2 value. Arrows indicate changes in mandibular shape from a weaker to stronger mandible. **A,** Dorsoventral bending force at the canine. **B,** Lateromedial bending force at the postcarnassial. **C,** Relative mandibular force at the canine. **D,** Mechanical advantage of the canine-temporalis lever system. **E,** Mechanical advantage of the carnassial-masseter lever system. **F,** Volumetric average stress from the canine load. **G,** Volumetric average stress from the carnassial load.

only significantly different for the carnassial bite and is not significantly different for the stress and strain from the canine bite (p-value = 0.27) (Table 3). This is also true for between-group differences, as there are significant differences in the carnassial bite stress between Feliformia and Caniformia (adjusted p-value < 0.01), Hyaenodonta and Caniformia (adjusted p-value < 0.01), Mesonychia and Caniformia (adjusted p-value = 0.01), and Metatheria and Caniformia (adjusted p-value < 0.01) (Table 4). The highest stress on the carnassial among the taxonomic grouping is with the non-carnivoran carnivoramorphans, followed by caniforms, hyaenodontans, metatherians, mesonychians, and oxyaenodontans. For larger cladistic groupings, carnivoramorphans still have the highest stress from the carnassial load followed by creodonts, metatherians, and mesonychians.

When regressed onto Procrustes-aligned shape data, stress and strain metrics are equally capable of explaining variation in shape $(R^2 \sim 0.12 \text{ and } p\text{-value} < 0.01 \text{ for both})$ and are comparable to the explanatory power of the mechanical advantage metric (Table 1). Canine loads are slightly better at explaining shape than the carnassial loads (the latter of which is $R^2 \sim 0.095$ and p-value < 0.01). PGLS of stress and strain data increases the R^2 value and maintains significance ($R^2 = 0.25$ for canine stress and $R^2 = 0.10$ for carnassial stress with both p-values < 0.01) (Table 2). Interactions between

these metrics and either ecology or phylogeny have low explanatory power. As stress on the mandible decreases, the shape of the mandible changes in that it undergoes shortening, becomes flatter ventrally, with a reduction in postcarnassial area and a more rostral-orientated masseteric fossa (Fig. 7F,G).

Convergence Testing

For bone-cracking taxa, there is evidence of overall convergence in stress from the canine bite with overall Ct1 = 33% and a taxonomic group weighted Ct1 = 42% (Table 5). For stress from the carnassial bite, bone-cracking taxa have weaker convergence with an overall Ct1 = 10% and a taxonomic group weighted Ct1 = 27%. When the stresses are considered together, overall Ct1 = 28% and taxonomic group weighted Ct1 = 38%. Looking at between-group differences, evidence of convergence from Ct1 with both stresses include Caniformia–Feliformia, Feliformia–Metatheria, Feliformia–Mesonychia, Feliformia–Oxyaenodonta, Mesonychia–Metatheria, and Metatheria—Oxyaenodonta, with Caniformia—Oxyaenodonta being the only divergent pairing.

For categorized hypercarnivorous taxa (non-bone-cracking taxa), there is evidence of divergence from the stress from the

Table 3. List of group means of the volumetric average von Mises stresses and effective Lagrange strain of the mandible from canine and carnassial loads with groups based on either ecology or clade.

Ecology	Average volumetric stress of scaled carnassial 100 N load (Pascals)	Average volumetric stress of scaled canine 100 N load (Pascals)
Hypocarnivore	3.77 × 10 ⁶	1.44 × 10 ⁷
Mesocarnivore	3.44 × 10 ⁶	1.70 × 10 ⁷
Bone-cracker	2.89 × 10 ⁶	1.19×10^{7}
Hypercarnivore	2.84 × 10 ⁶	1.51×10^{7}
<i>p</i> -value	0.07	<0.01
Clade		
Carnivoramorpha	4.05 × 10 ⁶	1.69 × 10 ⁷
Caniformia	3.87×10^{6}	1.54×10^{7}
Feliformia	2.84 × 10 ⁶	1.41 × 10 ⁷
Hyaenodonta	2.59 × 10 ⁶	1.64 × 10 ⁷
Metatheria	2.45 × 10 ⁶	1.60 × 10 ⁷
Mesonychia	2.33 × 10 ⁶	1.26 × 10 ⁷
Oxyaenodonta	1.98 × 10 ⁶	9.48 × 10 ⁶
<i>p</i> -value	<0.01	0.27

canine bite for both overall and taxonomic group weighted Ct1 (i.e., Ct1 < 0). Similar results of divergence are found with the stress from the carnassial bite for both overall and taxonomic group weighted Ct1. When the stresses are considered together, there is still evidence of divergence from overall and taxonomic group weighted Ct1. Looking at between-group differences, evidence of convergence between groups includes Feliformia—Hyaenodonta, Feliformia—Oxyaenodonta, Caniformia—Hyaenodonta, Caniformia—Oxyaenodonta, and Hyaenodonta—Oxyaenodonta. Evidence of divergence is in the remaining possible between groups (e.g., Caniformia—Feliformia) (Supplementary Table S2).

Discussion

Biomechanical Drivers of Shape

Comparative rates of shape evolution showed that the ascending ramus (the posterior portion of the mandible with muscular attachments) undergoes higher rates of evolutionary change in morphology than the horizontal ramus of the mandible. The ascending ramus is associated with the insertion of the abductor masticatory muscles such as the temporalis and the masseter. The orientation and proportional size of these masticatory muscles would highly influence the shape of the ascending ramus. For example, the shape of the coronoid process would be related to the temporalis muscles and the masseteric fossa and the angular process to the masseter muscles (Ross et al. 2005; Hart et al. 2017; Perry and Prufrock 2018; Hartstone-Rose et al. 2019, 2022). The shape of the horizontal ramus would likely be influenced by toothrow length and the functional demands of the mandible for certain ecologies such as length for capturing prey or depth and thickness to resist strong forces in biting. If this is the case, it would be likely that functional and biomechanical metrics more associated with the ascending ramus, such as masticatory muscle size and orientation, would have greater explanatory power on the variation of morphology of the mandible.

Table 4. List of between-group pair comparisons of the volumetric average von Mises stresses of the mandible from canine and carnassial loads within ecological and taxonomic groups from a Tukey post hoc test. Numbers in bold show significant differences between groups.

Ecology pairs	Canine stress adjusted <i>p</i> -value	Carnassial stress adjusted <i>p</i> -value	
Hypercarnivore/bone-cracker	0.07	1.00	
Hypocarnivore/bone-cracker	0.62	0.34	
Mesocarnivore/bone-cracker	<0.01	0.30	
Hypocarnivore/hypercarnivore	0.98	0.26	
Mesocarnivore/hypercarnivore	0.29	0.15	
Mesocarnivore/hypocarnivore	0.52 0.91		
Taxonomic pairs			
Carnivoramorpha/Caniformia	1.00	1.00	
Feliformia/Caniformia	0.95	<0.01	
Hyaenodonta/Caniformia	1.00	<0.01	
Mesonychia/Caniformia	0.81	0.01	
Metatheria/Caniformia	1.00	<0.01	
Oxyaenodonta/Caniformia	0.58	0.13	
Feliformia/Carnivoramorpha	0.92	0.26	
Hyaenodonta/Carnivoramorpha	1.00	0.16	
Mesonychia/Carnivoramorpha	0.77	0.11	
Metatheria/Carnivoramorpha	1.00	0.08	
Oxyaenodonta/Carnivoramorpha	0.51	0.20	
Hyaenodonta/Feliformia	0.85	0.99	
Mesonychia/Feliformia	0.99	0.92	
Metatheria/Feliformia	0.90	0.92	
Oxyaenodonta/Feliformia	0.82	0.90	
Mesonychia/Hyaenodonta	0.67	1.00	
Metatheria/Hyaenodonta	1.00	1.00	
Oxyaenodonta/Hyaenodonta	0.47	0.98	
Metatheria/Mesonychia	0.73	1.00	
Oxyaenodonta/Mesonychia	0.98	1.00	

Linear regression of the metrics on shape showed that, on average, the mechanical advantage measurements have higher explanatory power than any of the beam analysis metrics. This greater explanatory power may be because the in-lever for the mechanical advantage measurements captures muscle orientation and input force and includes the ascending ramus in its calculations. However, of all the functional metrics used, average von Mises stress on the mandible had the highest explanatory power, because FEA captures the average von Mises stress by volume of the entire mandible. This would mean that von Mises stress measurements had a greater representation of the mandibular shape than the mechanical advantage, which reduces mandibular shape to the in-lever and out-lever of the mandible.

Table 5. Printed *Ct1* measures from the convergence testing of the volumetric average von Mises stresses for canine and carnassial among bone-crackers and hypercarnivores of taxonomic groups. Bold highlights overall values.

E	Bone-cracker	rs	
Overall and taxonomic pairs	Ct1 of canine stress	Ct1 of carnassial stress	Ct1 of canine and carnassial stress
Overall	33%	10%	28%
Caniformia/Feliformia	6%	-12%	0.3%
Feliformia/Metatheria	54%	62%	52%
Feliformia/Mesonychia	76%	74%	75%
Feliformia/Oxyaenodonta	59%	54%	57%
Caniformia/Metatheria	16%	-10%	3%
Caniformia/Mesonychia	43%	-10%	37%
Caniformia/Oxyaenodonta	-33%	-63%	-39%
Mesonychia/Metatheria	67%	53%	65%
Metatheria/Oxyaenodonta	54%	52%	52%
Mesonychia/Oxyaenodonta	80%	73%	79%
Overall weighted	42%	27%	38%
H	ypercarnivor	res	
Overall and taxonomic pairs	Ct1 of canine stress	Ct1 of carnassial stress	Ct1 of canine and carnassial stress
Overall	-203%	-242%	-203%
Caniformia/Feliformia	-13%	18%	-12%
Feliformia/Metatheria	-395%	-301%	-395%
Feliformia/Mesonychia	-397%	-47%	-364%
Feliformia/Hyaenodonta	20%	-40%	15%
Feliformia/Oxyaenodonta	66%	66%	66%
Carnivoramorpha/Feliformia	-1026%	-780%	-1,012%
Caniformia/Metatheria	-135%	-282%	-148%
Caniformia/Mesonychia	-198%	-11%	-182%
Caniformia/Hyaenodonta	42%	-36%	33%
Caniformia/Oxyaenodonta	13%	27%	13%
Caniformia/Carnivoramorpha	-655%	-512%	-648%
Mesonychia/Metatheria	-749%	-906%	-774%
Hyaenodonta/Metatheria	-248%	-549%	-263%
Metatheria/Oxyaenodonta	-526%	-579%	-526%
Carnivoramorpha/Metatheria	-459%	-781%	-468%
Hyaenodonta/Mesonychia	-219%	-111%	-206%
Mesonychia/Oxyaenodonta	-468%	-144%	-437%
Carnivoramorpha/Mesonychia	-50%	-105%	-62%
Hyaenodonta/Oxyaenodonta	23%	23%	22%
Carnivoramorpha/Hyaenodonta	a -850%	-205%	-657%
Carnivoramorpha/Oxyaenodon	ta —1415%	-323%	-1083%

For the beam analysis, the measurements around the canine had higher R^2 values on shape than in other areas of the mandible (Table 1). This is also true for the finite element analysis, as the average stress of the mandible at the canine had a higher R^2 than at the main carnassial. The increase in explanatory power for metrics around the canine may be due to the fact that the rostral portion of the mandible that includes the canine is associated with prey capture or subduing (i.e., the "throat-bite" of large felids; Van Valkenburgh 1999, 2007), which, given the size of the carnivore and its typical prey size, could result in different shapes in that portion of the mandible for different functions or lifestyles.

However, the situation is more complex for the mechanical advantage measurements, as the canine-temporalis had better explanatory power than carnassial-masseter, but the latter had higher explanatory power than canine-masseter. This difference could be due to the different demands associated with the canine and molars and the respective masticatory muscles. In carnivores, the temporalis is often the larger of the two muscle groups, with its main purpose being for mandible elevation to produce a strong bite force, whereas the masseter is used for elevation and side-to-side motion in conjunction with the medial pterygoid muscles (Tseng et al. 2011; Perry and Prufrock 2018; Hartstone-Rose et al. 2022). The side-to-side motion is more likely to be experienced with the function of the molars to process foods, whereas the canines are more associated with prey capture via closing. Additionally, to fully occlude jaws, side-to-side movement must be quite limited, so the upper and lower canines can slide past each other. The canines being associated with prey capture via closing may also provide an explanation as to why average volumetric stress on the mandible via the canine bite better explains shape. Many therian carnivores acquire prey with their jaws and need to be able to handle the forces caused by struggling prey (Christiansen and Adolfssen 2005).

Generally, a biomechanically stronger jaw (in this case, greater resistance to bending, torsion, and stress, and better transmitting muscle force) is associated with jaw shape that exhibited shortening, greater depth, greater areas of muscle attachment (including coronoid height and the rostral extent of the masseter), and an increase in carnassial blade length (Fig. 6). These features are generally adaptations for a more hypercarnivorous or bonecracking ecology (or higher bite forces in general; Christiansen 2008; Prevosti et al. 2012; Echarri et al. 2017), such as the hypercarnivorous mustelids (e.g., Mustela nivalis, Gulo gulo), the mesonychids, and felids (e.g., Pseudaelurus) from this study. In this study, many of the taxa that are hypercarnivorous shared these features of a stronger jaw, a greater mandibular depth, greater areas of muscle attachment (temporalis with the coronoid process or deep masseter with the mandibular fossa), increases in carnassial blade length, and shortening of the mandible. For the last one, this is more apparent in Carnivoramorpha and Metatheria such as Pseudaelurus and Arctodictis, respectively, than in the other groups, but is noticeable in Mesonychia with *Mongolestes*. In short, it appears that these results confirm that some biomechanical functions, such as stress on the mandible and the mechanical advantage of the canine and the temporalis muscle, do converge with diet type.

Phylogeny and Many-to-One Function in Carnivory

Mandibular shape is more strongly correlated with taxonomy and phylogenetic history than with its ecological role, and this correlation is reflected in the PCA of the shape of the mandible (Figs. 4, 5).

This correlation with phylogenetic history had been shown to be the case in a prior study by Meloro and O'Higgins (2011) using 2D geometric morphometrics on the mandibles of "fissiped" carnivorans. Influences of this may be due to characteristics such as carnassial placement, as "creodonts" and metatherians have their main carnassial positioned more posteriorly than carnivorans and the "carnassial" for mesonychids was placed more posteriorly in landmark placing. Greaves (1983) found that carnassial placement in Carnivora is based on the optimization of mechanical advantage to have the highest force while having room for food. Non-carnivoran carnivores such as metatherians and creodonts still hold to this principle to an extent with longer mandibles. Another influence on mandibular shape regarding carnassial length in Carnivoramorpha is that there was an early diversification into several carnassial types that are strongly associated with extant family-level clades (e.g., Canidae, Felidae, Mustelidae; Hopkins et al., 2022). While taxonomy better explains the differences in mandibular shape in the taxa of this study, the explanatory power of the biomechanical metrics on shape that is within the normal means of the explanation of function on morphology captured by geometric morphometrics, as shown in a study on marmot mandibles by Caumul and Polly (2005). While phylogenetic history has a large role in shaping mandibular evolution, functionality is still an influence and may have a greater one in lower clades.

In Figure 4, categorized ecological groups such as hypercarnivores and bone-crackers occupied a large portion of morphospace. This large occupation of morphospace may indicate that there are many ways in which deeply phylogenetically separated groups of therian carnivores achieved specialized ecologies such as hypercarnivory and bone-cracking in mandibular shape despite phylogenetic constraints. In this case, evolutionary starting points that may influence the variation available in mandibular shape are likely to be ancestral dental formula and shape. Examples of this include metatherians having four lower molars and three premolars as opposed to three molars and four premolars in eutherians, mesonychians being ancestrally omnivorous or herbivorous and losing their shearing surface through their evolutionary history (Szalay 1969), creodonts having all their lower molars carnassialized, and carnivoramorphans only having one carnassialized molar. However, the data were still generally able to separate the ecologies by their biomechanical metrics such as von Mises stress from loads on the mandible, although this is truer in the canine when looking between bonecrackers and mesocarnivores following a Tukey post hoc test. This separation of ecologies could indicate that there are common functional requirements still required for these ecologies, but these can be fulfilled by different mandibular shapes.

Alongside the results of the PCA of shape seen in Figure 4, it appears that bone-crackers of different shapes have indeed converged on similar amounts of stress on the mandible, although more so with canine biting versus carnassial biting. This could be interpreted as evidence of a many-to-one form–function relationship of the mandibles of bone-cracking carnivores, as many shapes are able to converge on similar amounts of reduced stress on the mandible. Between-group difference analysis supported this, as most taxonomic groups with bone-cracking carnivores showed convergence among one another, except for certain Caniformia pairings depending on canine stress or carnassial stress.

However, non-bone-cracking hypercarnivores overall showed divergence and did not strongly indicate many-to-one mapping of mandibular form and function. The divergence in stress among non-bone-cracking hypercarnivores could be attributed to

phylogenetic history in mandibular shape and ancestral tooth count and diet, as mentioned previously. Between-group differences showed convergence in stress results among some taxonomic groups that have a true carnassial on the last tooth (Feliformia, Hyaenodonta, and Oxyaenodonta) or have three molars that include at least one true carnassial (Caniformia and Hyaenodonta). These three groups occupied distinct areas of morphospace on the first PCs (Fig. 5). It could be interpreted that hypercarnivory may have many-to-one mapping for these specific groups. However, the lack of significant between-group differences in carnassial stress between ecological groups should be noted with this interpretation, and additional analyses among these groups may be necessary.

Another aspect to note is that, with the large phylogenetic sampling, the mesocarnivores may be a group of generalists that have different shapes among them. Aspects of morphological shape that would be expected to be shared among generalist mesocarnivores would include a rostrocaudally longer and dorsoventrally shallower horizontal ramus in comparison to the length of the mandible (Van Valkenburgh et al. 2004; Van Valkenburgh 2007; Prevosti et al. 2012; Echarri et al. 2017); this feature could also be a feature of small prey specialist hypercarnivores (Mitchell et al. 2024; Sansalone et al. 2024). However, it should also be noted that mesocarnivores may have variation between one another in the portion of their diet that is non-vertebrate material (i.e., one mesocarnivore might supplement that diet with more invertebrate material, while another mesocarnivore supplements it with more fruit or seeds) and have different morphological adaptations accordingly. It could be possible to look at the heterogeneity of mesocarnivores further with a larger sample of mesocarnivores with known differences in the non-vertebrate portion of their respective diets.

Conclusion

We tested a hypothesis of parallelism and many-to-one mapping of form to function in carnivore jaws and predicted that species that are ecologically similar will have similar patterns of stress and strain on the mandible even if they plot separately on mandibular morphospace. Our analyses showed that even though the form of the mandible is phylogenetically varied for any given dietary group, there is indeed convergence in biomechanical function as measured by stress and strain for bone-cracking specialists and certain groups of hypercarnivores such as Feliformia, Hyaenodonta, Oxyaenodonta, and sometimes Caniformia. We found that even though mandibular shape tended to be distinctive in the more derived ecological groups and that there was some degree of evolutionary convergence on those forms and functions, the shape groupings tended to be more taxonomic than ecological. Hypercarnivores and bone-crackers tend to plot in far spaces of morphospace based on the first two principal components. The dietary groups tend to reach certain areas in the morphospace for the first three PCs, but there are some phylogenetic distinctions within groups observed, such as "Creodonta" clustering together in a small part of the mesocarnivore cluster, but carnivorans being widely dispersed. It should be noted that mesocarnivores occupying the center of the first PC is not indicative that they are similar to the overall mean shape of the mandibles. The large morphospace occupation of hypercarnivores and bone-crackers may be indicative of different shapes in mandibles that can be effective at occupying a highly carnivorous ecologic niche. This is partially supported by the convergence testing of stress in bone-crackers and certain hypercarnivore groups. Additionally, generally early taxa categorized as

mesocarnivorous tend to have higher stress on the mandible than later hypercarnivorous taxa in their respective lineages.

Nevertheless, there are still some common biomechanical traits that influence mandibular shape for certain niches, such as a trend of shortening of the mandible and increase in jaw muscle areas such as the ascending ramus in the evolution toward hypercarnivory. Biomechanical factors that are better at explaining mandibular shape are those that use the ascending ramus as a part of its metric, such as mechanical advantage and stress and strain on the mandible. Typically, a higher mechanical advantage and lower stress on the mandible are indicative of a mandibular shape that is typical of a hypercarnivorous diet and that can both transmit the force from the closing jaws more effectively and better resist those forces. Additionally, biomechanical factors that involve the canine have greater explanatory power due to the variability in that area for capturing and subduing prey.

Acknowledgments. The authors would like to acknowledge the various curators and museum workers who helped make data collection possible during the COVID-19 pandemic.

Competing Interests. The authors of this paper have no competing interests.

Data Availability Statement. Supplementary Fig. S1, Tables S1 and S2, and the therian mandible code are available on Dryad at https://doi.org/10.5061/dryad.d7wm37qd7 and Zenodo at https://doi.org/10.5281/zenodo.15882751.

Funding Statement. Funding sources include the Indiana University Earth and Atmospheric Sciences Galloway/Perry/Horowitz Fellowship and the AmeriCorps Education Award.

Literature Cited

- Adams, D., M. Collyer, A. Kaliontzopoulou, and E. Baken. 2023. Geometric morphometric analysis of 2D and 3D landmark data, R package version 4.0.5. https://cran.r-project.org/package=geomorph.
- Adams, D. C., and M. L. Collyer. 2018. Multivariate phylogenetic comparative methods: evaluations, comparisons, and recommendations. Systematic Biology 67:14–31.
- Adams, D. C., and E. Otárola-Castillo. 2013. geomorph: an R package for the collection and analysis of geometric morphometric shape data. *Methods in Ecology and Evolution* 4:393–399.
- Adams, D. C., F. J. Rohlf, and D. E. Slice. 2004. Geometric morphometrics: ten years of progress following the "revolution." *Italian Journal of Zoology* 71:5–16.
- Ahrens, H. E. 2017. Phylogeny and locomotor ecomorphology of Oxyaenidae and macroevolutionary patterns in North American "Creodonta" (Mammalia, Placentalia). PhD dissertation. Johns Hopkins University, Baltimore, Md.
- Alfaro, M. E., D. I. Bolnick, and P. C. Wainwright. 2005. Evolutionary consequences of many-to-one mapping of jaw morphology to mechanics in labrid fishes. *American Naturalist* 165:E140–E154.
- Balisi, M., C. Casey, and B. Van Valkenburgh. 2018. Dietary specialization is linked to reduced species durations in North American fossil canids. *Royal Society Open Science* 5(4):171861.
- Baskin, J. A. 1998. 9 Mustelidae. Pp. 152–173 in C. M. Janis, K. M. Scott, and L. L. Jacobs, eds. Evolution of Tertiary mammals of North America. Vol. 1, Terrestrial carnivores, ungulates, and ungulatelike mammals. Cambridge University Press, Cambridge.
- Benevento, G. L., R. B. Benson, and M. Friedman. 2019. Patterns of mammalian jaw ecomorphological disparity during the Mesozoic/Cenozoic transition. *Proceedings of the Royal Society B* **286**:20190347.
- Biknevicius, A., and C. Ruff. 1992. The structure of the mandibular corpus and its relationship to feeding behaviours in extant carnivorans. *Journal of Zoology* 228:479–507.
- Borths, M. R., P. A. Holroyd, and E. R. Seiffert. 2016. Hyainailourine and teratodontine cranial material from the late Eocene of Egypt and the

- application of parsimony and Bayesian methods to the phylogeny and biogeography of Hyaenodonta (Placentalia, Mammalia). PeerJ 4:e2639.
- Bright, J. A. 2014. A review of paleontological finite element models and their validity. *Journal of Paleontology* 88:760–769.
- Bright, J. A., and F. Gröning. 2011. Strain accommodation in the zygomatic arch of the pig: a validation study using digital speckle pattern interferometry and finite element analysis. *Journal of Morphology* 272:1388–1398.
- Brightly, W., and T. Stayton. 2024. Analysis of convergent evolution, R package version 2.2.1. https://cran.r-project.org/package=convevol.
- Brito, A. 2007. Blender 3D. Novatec, New York.
- Butler, P. 1946. The evolution of carnassial dentitions in the Mammalia. Proceedings of the Zoological Society of London 116:198–220.
- Caumul, R., and P. D. Polly. 2005. Phylogenetic and environmental components of morphological variation: skull, mandible, and molar shape in marmots (Marmota, Rodentia). Evolution 59:2460–2472.
- **Christiansen, P.** 2008. Evolution of skull and mandible shape in cats (Carnivora: Felidae). *PLoS ONE* 3(7):e2807.
- Christiansen, P., and J. S. Adolfssen. 2005. Bite forces, canine strength and skull allometry in carnivores (Mammalia, Carnivora). *Journal of Zoology* 266: 133–151.
- Cignoni, P., M. Callieri, M. Corsini, M. Dellepiane, F. Ganovelli, and G. Ranzuglia. 2008. Meshlab: an open-source mesh processing tool. Pp. 129–136 *in* Eurographics Italian Chapter Conference. https://diglib.eg.org/server/api/core/bitstreams/eb20f1e6-5138-42bf-8b32-f4326a619969/content.
- **Crompton, A., and K. Hiiemae**. 1969. How mammalian molar teeth work. *Discovery* **5**:23–34.
- Currey, J. 1984. Comparative mechanical properties and histology of bone. American Zoologist 24:5–12.
- Denton, J. S. S., and D. C. Adams. 2015. A new phylogenetic test for comparing multiple high-dimensional evolutionary rates suggests interplay of evolutionary rates and modularity in lanternfishes (Myctophiformes; Myctophidae). Evolution 69:2425–2440.
- Dumont, E., I. R. Grosse, and G. J. Slater. 2009. Requirements for comparing the performance of finite element models of biological structures. *Journal of Theoretical Biology* 256:96–103.
- Echarri, S., M. D. Ercoli, M. A. Chemisquy, G. Turazzini, and F. J. Prevosti. 2017. Mandible morphology and diet of the South American extinct metatherian predators (Mammalia, Metatheria, Sparassodonta). *Transactions of the Royal Society of Edinburgh (Earth Sciences)* 106: 277–288.
- Gill, P. G., M. A. Purnell, N. Crumpton, K. R. Brown, N. J. Gostling, M. Stampanoni, and E. J. Rayfield. 2014. Dietary specializations and diversity in feeding ecology of the earliest stem mammals. *Nature* 512:303–305.
- Goin, F. J., M. O. Woodburne, A. N. Zimicz, G. M. Martin, and L. Chorno-gubsky. 2016. Dispersal of vertebrates from between the Americas, Antarctica, and Australia in the Late Cretaceous and Early Cenozoic. In A brief history of South American Metatherians. Springer Earth System Sciences. Springer, Dordrecht, Netherlands, pp. 77–124.
- Goswami, A., N. Milne, and S. Wroe. 2011. Biting through constraints: cranial morphology, disparity and convergence across living and fossil carnivorous mammals. *Proceedings of the Royal Society B* 278:1831–1839.
- Greaves, W. 1983. A functional analysis of carnassial biting. Biological Journal of the Linnean Society 20:353–363.
- Greaves, W. 1985. The generalized carnivore jaw. Zoological Journal of the Linnean Society 85:267–274.
- Grossnickle, D. M., W. H. Brightly, L. N. Weaver, K. E. Stanchak, R. A. Roston, S. K. Pevsner, C. T. Stayton, P. D. Polly, and C. J. Law. 2024. Challenges and advances in measuring phenotypic convergence. *Evolution* 78:1355–1371.
- Halliday, T. J., P. Upchurch, and A. Goswami. 2017. Resolving the relationships of Paleocene placental mammals. *Biological Reviews* 92:521–550.
- Halliday, T. J. D., and A. Goswami. 2016. Eutherian morphological disparity across the end-Cretaceous mass extinction. *Biological Journal of the Linnean Society* 118:152–168.
- Hart, N. H., S. Nimphius, T. Rantalainen, A. Ireland, A. Siafarikas, and R. Newton. 2017. Mechanical basis of bone strength: influence of bone material, bone structure and muscle action. *Journal of Musculoskeletal and Neuronal Interactions* 17:114.

- Hartstone-Rose, A., I. Hertzig, and E. Dickinson. 2019. Bite force and masticatory muscle architecture adaptations in the dietarily diverse Musteloidea (Carnivora). Anatomical Record 302:2287–2299.
- Hartstone-Rose, A., E. Dickinson, A. R. Deutsch, N. Worden, and G. A. Hirschkorn. 2022. Masticatory muscle architectural correlates of dietary diversity in Canidae, Ursidae, and across the order Carnivora. *Anatomical Record, part A* 305:477–497.
- Hopkins, S. S., S. A. Price, and A. J. Chiono. 2022. Influence of phylogeny on the estimation of diet from dental morphology in the Carnivora. *Paleobiology* 48:324–339.
- Huberty, C. J., and M. D. Petoskey. 2000. Multivariate analysis of variance and covariance. Pp. 183–208 in H. E. A. Tinsley and S. D. Brown, eds. Handbook of applied multivariate statistics and mathematical modeling. Academic Press, San Diego.
- Hunt, R. M., Jr. 1998. Evolution of the aeluroid Carnivora. Diversity of the earliest aeluroids from Eurasia (Quercy, Hsanda-Gol) and the origin of felids. *American Museum Novitates*, no. 3252.
- Ihaka, R., and R. Gentleman. 1996. R: a language for data analysis and graphics. Journal of Computational and Graphical Statistics 5:299–314.
- Kitchener, A. C., B. Van Valkenburgh, N. Yamaguchi, D. Macdonald, and A. Loveridge. 2010. Felid form and function. *Biology and Conservation of Wild Felids* 2010:83–106.
- Losos, J. B. 2011. Convergence, adaptation, and constraint. Evolution 65: 1827–1840.
- Maas, S. A., B. J. Ellis, G. A. Ateshian, and J. A. Weiss. 2012. FEBio: finite elements for biomechanics. *Journal of Biomechanical Engineering* 134(1): 011005.
- Marcé-Nogué, J., S. De Esteban-Trivigno, T. A. Püschel, and J. Fortuny. 2017.
 The intervals method: a new approach to analyse finite element outputs using multivariate statistics. *PeerJ* 5:e3793.
- Marinescu, R., D. J. Daegling, and A. J. Rapoff. 2005. Finite-element modeling of the anthropoid mandible: the effects of altered boundary conditions. *Anatomical Record, part A* **283**:300–309.
- Martin, L. D. 1989. Fossil history of the terrestrial Carnivora. Pp. 536–568 in John L. Gittleman, ed. Carnivore behavior, ecology, and evolution. Springer Science+Business Media, Dordrecht, Netherlands.
- **Meachen-Samuels, J., and B. Van Valkenburgh.** 2009. Craniodental indicators of prey size preference in the Felidae. *Biological Journal of the Linnean Society* **96**:784–799.
- Meloro, C., and P. O'Higgins. 2011. Ecological adaptations of mandibular form in fissiped Carnivora. *Journal of Mammalian Evolution* 18:185–200.
- **Meloro, C., and P. Raia.** 2010. Cats and dogs down the tree: the tempo and mode of evolution in the lower carnassial of fossil and living Carnivora. *Evolutionary Biology* 37:177–186.
- Meloro, C., M. Clauss, and P. Raia. 2015. Ecomorphology of Carnivora challenges convergent evolution. *Organisms Diversity and Evolution* 15: 711–720.
- Metzger, K. A., W. J. Daniel, and C. F. Ross. 2005. Comparison of beam theory and finite-element analysis with in vivo bone strain data from the alligator cranium. *Anatomical Record*, part A 283:331–348.
- Mitchell, D. R., E. Sherratt, and V. Weisbecker. 2024. Facing the facts: adaptive trade-offs along body size ranges determine mammalian craniofacial scaling. *Biological Reviews* **99**:496–524.
- Morales-García, N. M., T. D. Burgess, J. J. Hill, P. G. Gill, and E. J. Rayfield. 2019. The use of extruded finite-element models as a novel alternative to tomography-based models: a case study using early mammal jaws. *Journal of the Royal Society Interface* 16(161):20190674.
- Perry, J. M., and K. A. Prufrock. 2018. Muscle functional morphology in paleobiology: the past, present, and future of "paleomyology." *Anatomical Record* 301:538–555.
- Peters, S. E., and M. McClennen. 2016. The Paleobiology Database application programming interface. *Paleobiology* 42:1–7.
- Pineda-Munoz, S., I. A. Lazagabaster, J. Alroy, and A. R. Evans. 2017. Inferring diet from dental morphology in terrestrial mammals. *Methods in Ecology and Evolution* 8:481–491.
- Porro, L. B., C. M. Holliday, F. Anapol, L. C. Ontiveros, L. T. Ontiveros, and C. F. Ross. 2011. Free body analysis, beam mechanics, and finite element

- modeling of the mandible of Alligator mississippiensis. *Journal of Morphology* **272**:910–937.
- Prevosti, F. J., G. F. Turazzini, M. D. Ercoli, and E. Hingst-Zaher. 2012. Mandible shape in marsupial and placental carnivorous mammals: a morphological comparative study using geometric morphometrics. Zoological Journal of the Linnean Society 164:836–855.
- Radinsky, L. B. 1982. Evolution of skull shape in carnivores. 3. The origin and early radiation of the modern carnivore families. *Paleobiology* 8:177–195.
- Rasband, W. S. 1997. ImageJ. NIH, Bethesda, Md.
- **Rayfield, E. J.** 2007. Finite element analysis and understanding the biomechanics and evolution of living and fossil organisms. *Annual Review of Earth and Planetary Sciences* **35**:541–576.
- Reed, D. A., L. B. Porro, J. Iriarte-Diaz, J. B. Lemberg, C. M. Holliday, F. Anapol, and C. F. Ross. 2011. The impact of bone and suture material properties on mandibular function in *Alligator mississippiensis*: testing theoretical phenotypes with finite element analysis. *Journal of Anatomy* 218:59–74.
- Renvoisé, E., K. D. Kavanagh, V. Lazzari, T. J. Häkkinen, R. Rice, S. Pantalacci, and J. Jernvall. 2017. Mechanical constraint from growing jaw facilitates mammalian dental diversity. Proceedings of the National Academy of Sciences USA 114:9403–9408.
- Revell, L. J. 2023. Phylogenetic tools for comparative biology (and other things), R package version 1.5-1. https://cran.r-project.org/package=phytools.
- Richmond, B. G., B. W. Wright, I. Grosse, P. C. Dechow, C. F. Ross, M. A. Spencer, and D. S. Strait. 2005. Finite element analysis in functional morphology. *Anatomical Record, part A* 283:259–274.
- Roemer, G. W., M. E. Gompper, and B. Van Valkenburgh. 2009. The ecological role of the mammalian mesocarnivore. *BioScience* **59**:165–173.
- Ross, C. F. 2005. Finite element analysis in vertebrate biomechanics. *Anatomical Record, part A* 283:253–258.
- Ross, C. F., B. A. Patel, D. E. Slice, D. S. Strait, P. C. Dechow, B. G. Richmond, and M. A. Spencer. 2005. Modeling masticatory muscle force in finite element analysis: sensitivity analysis using principal coordinates analysis. Anatomical Record, part A 283:288–299.
- Sansalone, G., S. Wroe, G. Coates, M. R. Attard, and C. Fruciano. 2024. Unexpectedly uneven distribution of functional trade-offs explains cranial morphological diversity in carnivores. *Nature Communications* 15(1):3275.
- Serrano-Fochs, S., S. De Esteban-Trivigno, J. Marcé-Nogué, J. Fortuny, and R. A. Fariña. 2015. Finite element analysis of the Cingulata jaw: an ecomorphological approach to armadillo's diets. PLoS ONE 10(4):e0120653.
- Slater, G., E. Dumont, and B. Van Valkenburgh. 2009. Implications of predatory specialization for cranial form and function in canids. *Journal of Zoology* 278:181–188.
- Solé, F., M. Godinot, Y. Laurent, A. Galoyer, and T. Smith. 2018. The European Mesonychid mammals: phylogeny, ecology, biogeography, and biochronology. *Journal of Mammalian Evolution* 25:339–379.
- Spaulding, M., and J. J. Flynn. 2012. Phylogeny of the Carnivoramorpha: the impact of postcranial characters. *Journal of Systematic Palaeontology* 10: 653–677.
- Stefen, C. 1997. The enamel of Creodonta, Arctocyonidae, and Mesonychidae (Mammalia), with special reference to the appearance of Hunter-Schreger-Bands. *Paläontologische Zeitschrift* 71:291–303.
- Strait, D. S., Q. Wang, P. C. Dechow, C. F. Ross, B. G. Richmond, M. A. Spencer, and B. A. Patel. 2005. Modeling elastic properties in finite-element analysis: how much precision is needed to produce an accurate model? *Anatomical Record, part A* 283:275–287.
- Stayton, C. T. (2015). The definition, recognition, and interpretation of convergent evolution, and two new measures for quantifying and assessing the significance of convergence. *Evolution*, 69(8), 2140–2153.
- Szalay, F. S. 1969. Origin and evolution of function of the mesonychid condylarth feeding mechanism. *Evolution* 23:703–720.
- Therrien, F. 2005. Mandibular force profiles of extant carnivorans and implications for the feeding behaviour of extinct predators. *Journal of Zoology* 267:249–270.
- **Tseng, Z. J.** 2013. Testing adaptive hypotheses of convergence with functional landscapes: a case study of bone-cracking hypercarnivores. *PLoS ONE* **8**(5): e65305
- Tseng, Z. J., and J. J. Flynn. 2015. Are cranial biomechanical simulation data linked to known diets in extant taxa? A method for applying diet-biomechanics

- linkage models to infer feeding capability of extinct species. PLoS ONE 10(4): e0124020
- Tseng, Z. J., and X. Wang. 2010. Cranial functional morphology of fossil dogs and adaptation for durophagy in Borophagus and Epicyon (Carnivora, Mammalia). *Journal of Morphology* 271:1386–1398.
- Tseng, Z. J., M. Antón, and M. J. Salesa. 2011. The evolution of the bone-cracking model in carnivorans: cranial functional morphology of the Plio-Pleistocene cursorial hyaenid *Chasmaporthetes lunensis* (Mammalia: Carnivora). *Paleobiology* 37:140–156.
- Tseng, Z. J., S. Garcia-Lara, J. J. Flynn, E. Holmes, T. B. Rowe, and B. V. Dickson. 2023. A switch in jaw form—function coupling during the evolution of mammals. *Philosophical Transactions of the Royal Society B* 378:20220091.
- Ungar, P. S. 2010. Mammal teeth: origin, evolution, and diversity. Johns Hopkins University Press, Baltimore, Md.
- Van Valkenburgh, B. 1988. Trophic diversity in past and present guilds of large predatory mammals. *Paleobiology* 14:155–173.
- Van Valkenburgh, B. 1991. Iterative evolution of hypercarnivory in canids (Mammalia: Carnivora): evolutionary interactions among sympatric predators. *Paleobiology* 17:340–362.
- Van Valkenburgh, B. 1999. Major patterns in the history of carnivorous mammals. Annual Review of Earth and Planetary Sciences 27:463–493.
- Van Valkenburgh, B. 2007. Déjà vu: the evolution of feeding morphologies in the Carnivora. *Integrative and Comparative Biology* **47**:147–163.
- Van Valkenburgh, B., X. Wang, and J. Damuth. 2004. Cope's rule, hypercarnivory, and extinction in North American canids. *Science* **306**:101–104.

- Varela, L., P. S. Tambusso, J. M. P. Zerpa, R. K. McAfee, and R. A. Fariña. 2023. 3D finite element analysis and geometric morphometrics of sloths (Xenarthra, Folivora) mandibles show insights on the dietary specializations of fossil taxa. *Journal of South American Earth Sciences* 128:104445.
- Wainwright, P. C., M. E. Alfaro, D. I. Bolnick, and C. D. Hulsey. 2005. Many-to-one mapping of form to function: a general principle in organismal design? *Integrative and Comparative Biology* 45:256–262.
- Werdelin, L., and J. Gittleman. 1996. Carnivoran ecomorphology: a phylogenetic perspective. Pp. 582–624 in John L. Gittleman, ed. Carnivore behavior, ecology, and evolution, Vol. 2. Cornell University Press, Ithaca, N.Y.
- Wesley-Hunt, G. D., and J. J. Flynn. 2005. Phylogeny of the Carnivora: basal relationships among the carnivoramorphans, and assessment of the position of 'Miacoidea' relative to Carnivora. *Journal of Systematic Palaeontology* 3: 1–28.
- Wozencraft, W. C. 1989. The phylogeny of the recent Carnivora. Pp. 495–535 in John L. Gittleman, ed. Carnivore behavior, ecology, and evolution. Springer Science+Business Media, Dordrecht, Netherlands.
- Wroe, S. 2008. Cranial mechanics compared in extinct marsupial and extant African lions using a finite-element approach. *Journal of Zoology* 274: 332–339.
- Wroe, S., C. McHenry, and J. Thomason. 2005. Bite club: comparative bite force in big biting mammals and the prediction of predatory behaviour in fossil taxa. *Proceedings of the Royal Society B* 272:619–625.